

oGoogleNet: An Optimized GoogleNet for ChestInfection Detection on the COVID-19 Dataset

Sumaira Zafar, Kanwal Majeed, Arjmand Majeed, Syed Farooq Ali*, and Aadil Zia Khan

School of Systems and Technology, University of Management and Technology, Lahore, Pakistan

ABSTRACT The outbreak of SARS and, more recently, COVID-19 has highlighted the need for accurate and quick diagnosis of chest diseases for pandemic prevention. While the handling of the COVID-19 pandemic has drawn attention to the weaknesses in the healthcare systems worldwide, it has also enabled us to fully utilize the massive amounts of data at our disposal in order to devise strategies for better handling outbreaks in the future. Chest infection is a crucial symptom used to diagnose COVID-19 cases. Moreover, it may also lead to various other diseases, including pneumonia, asthma, and bronchitis. Researchers have been working on automatic chest infection detection for the last few decades. In this study, we present oGoogleNet, a deep learning architecture for chest infection detection, developed by optimizing GoogleNet through the addition of layers and the modification of activation functions. The oGoogleNet is compared with the existing state-of-the-art deep networks on eight standard chest infection datasets, containing 12,389 radiographs (with 777 COVID-19 radiographs). The experiments demonstrate that oGoogleNet outperforms the other systems and achieves an accuracy of 91.25%.

INDEX TERMS Convolution's Neural Networks (CNN), Deep Learning (DL), oGoogleNet

I. INTRODUCTION

The COVID-19 pandemic has disrupted the world's economy in a way not seen in the recent past. The economies are on the verge of collapse worldwide. Unemployment rate has shot up drastically, GDP growth has been adversely affected, and there has been an increase in deaths caused by both COVID-19 as well as subsequent lock-down-related suicides [1]. In short, the abrupt and rapid spread of the novel virus has caused massive uncertainty. On March 18th 2020, the International Labor Organization reported a 4.936-5.644% increase in the unemployment rate worldwide [2]. It further said that this increased rate would also increase the

suicide ratio from 2135 to 9570 per year, respectively. Their previous study is based on public data from 63 countries. Furthermore, suicide risk has increased now by 20-30% as compared to the last decade, especially during the 2008 recession [3].

Coibion et al. in 2020 reported extraordinarily high figures of unemployment, that is, 16.5 million due to the COVID-19 virus [4]. They predicted an increase of 6-7 million per week in the unemployment rate starting from April 2020. As compared to the pre-COVID-19 condition, the percentage increase in the rate of unemployment is 12.2% as 20

*Corresponding Author: farooq.ali@umt.edu.pk

million people lost their jobs.

The scale of COVID-19's socio-economic impact is enormous as compared to the past era's pandemic. For instance, H5NA (Avian Influenza) was caused by poultry-hum interaction and it caused 400 deaths in 2008 [5]. The Middle East Respiratory Syndrome (MERS) epidemic caused more than 400 deaths in the Middle East in 2012 and 150 deaths in South Korea in 2015 [6].

During the COVID-19 pandemic, the USA's death rate has been 0.02% as of June 1st, 2020 [6]. From February 29th 2020 to June 5th 2020 in England, around 23.6% (44,736) deaths were registered as COVID-19-related. For Wales, in the same period, the figure was close to 20.3% (2,294) [7]. The country-wise death rate from pneumonia, grouped by age from 2010 to 2017, is shown in Figure 1¹.

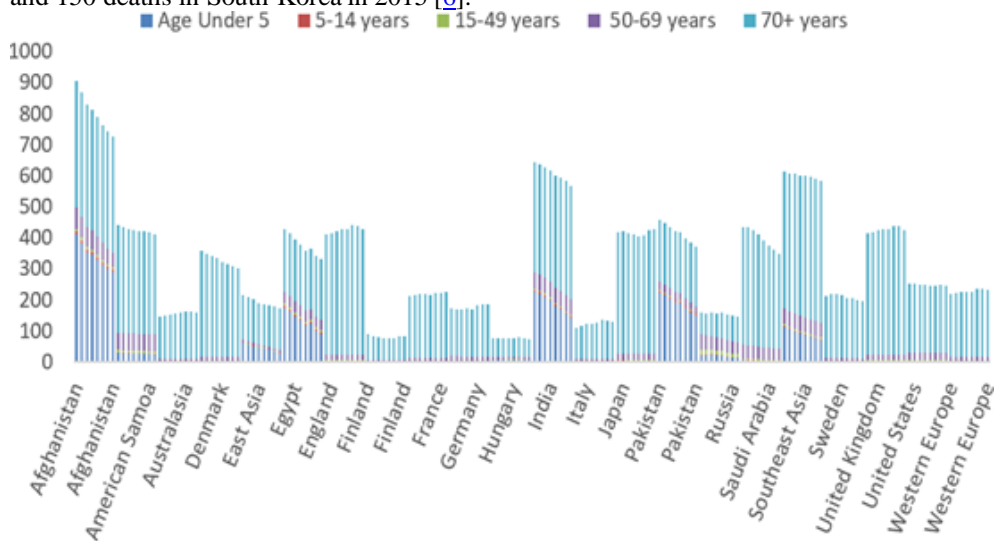


FIGURE 1. World death rate caused by pneumonia from 2010 to 2017

Nowadays, there is an urgency to find effective mechanisms for the diagnosis and treatment of COVID-19 pandemic. It is a multifaceted re-search effort bringing in scientists from diverse fields including health, pharmaceuticals, and ML and data sciences. Still, other rooms are open for technical visions and resolution of this pandemic in Artificial Intelligence (AI), Deep Learning (DL), and big data [8]. Careful testing, accurate diagnosis, and proper treatment are essential in this current COVID-19 pandemic. The RT-PCR (Reverse transcription-polymerase chain

reaction) is an important examination for COVID-19 [9]. A quick, efficient, and economically reasonable test for this pandemic is chest radiographs. It detects pneumonia symptoms, which reflect the possibility of the coronavirus [10]. Chest radiographs illustrate visual guidance related to COVID-19 pandemic [11].

The study of a chest radiograph is a challenging task. It is error-prone and requires an expert system that can assist pathologists in properly diagnosing it [12]. Each year, millions of people develop

¹<https://ourworldindata.org/grapher/pneumonia-mortality-by-age?year=latest>

thoracic diseases, such as lung cancer and tuberculosis. An accurate interpretation of a chest radiograph is very crucial to diagnose these diseases. The process of interpreting the radiographs is time-consuming and does not allow much margin for error. In recent years, DL-based radiograph interpretation seems to bring promising results. In the case of DL, feature extraction is performed in a different but systematic way, requiring lesser human intervention [13].

This study proposed a DL architecture, oGoogleNet. This automatically detects abnormalities in radiographs, especially from COVID-19 datasets and assists in automated interpretation of the disease. Large data set of chest radiographs from different sources have been used to train and test this algorithm. The classification accuracy and running time of the approach are compared with other state-of-the-art Deep Learning Algorithms (DLA's) including AlexNet, Inception-V3, ResNet-152, and VGG16.

The remainder of the paper is organized as follows: Section II describes the related work, while Section III explains the proposed methodology. Section IV describes the dataset. Section V presents various experiments of oGoogleNet using different datasets, while the conclusion and future work are given in Section VI.

II. RELATED WORK

In July 2020, Yoo et al. examined the diagnostics of COVID-19 from CXR images by applying a Decision Tree (DT) classifier based on DL [14]. The classifier presented in the study comprised three binary tree classifiers. Each tree's training was done by applying a PyTorch-based DL model with a Convolutional Neural network (CNN). The first and second DTs yielded an accuracy of 98% and 80%,

respectively, while the third DT achieved 95%. The DT classifier, based on DL, may be applied for rapid decision-making and for carrying out triage in pre-diagnostic testing of patients when the results of RT-PCR are delayed.

In 2018, Razzak et al. discussed the modern and cutting-edge architecture and optimization of DLAs [15]. The disease, that is, Diabetic Retinopathy (DR), can be detected and classified using Deep Convolutional Neural Network (DCNN) at its initial stages [16]. Moreover, DCNN can also be used to detect colon cancer nuclei cells using histological images [17]. CNN has also been applied for the extraction of features from endoscopy images [18]. This diagnostic process has 80% accuracy. There is also a need to develop techniques in order to handle a tremendously large quantum of data relating to the healthcare system. Since access to the annotated dataset is not familiar and comfortable, the data resources must be shared with various service providers of healthcare.

In the year 2020, Peng et al. forecasted the top 12 countries severely affected by the quantum of COVID-19 cases by utilizing the support vector regression [19]. Various non-linear assemblies were tested by applying Kernel functions. While 3-D interpolated surfaces were used to carry out the sensitivity analysis of the model's performance regarding their forecasting ability. These results helped in the practical evaluation of basic data analysis concepts. Moreover, it was also demonstrated that attentiveness is required while using Machine Learning (ML) models to support decision-making in the real world regarding the COVID-19 challenges. Liu et al. proposed an excellent optimized model of CNN architectures [20]. However, it has a problem with the pre-processing of data.

Esteva et al. proposed a model to rectify two types of skin cancers, common and deadly, in clinical skincare images [21]. Rajpurkar et al. proposed a model for the detection of pneumonia that contains 121 CNN layers [22]. Murphey et al. selected chest radiographs from Jeroen Bosch Hospital and used AI classifier to identify COVID- pneumonia with 81% accuracy [23]. However, they collected the whole data from a single institute.

Ming et al. proposed a literature review of the COVID-19 pandemic using test cases of chest radiographs from Shenzhen Hospital [24]. Chest radiographs were reviewed by two radiologists. Another technique to detect COVID-19 was proposed by Alqudah et al. [25]. Their research was based on ML, where they implemented the Support Vector Machine (SVM), K-nearest neighbor, random forest, and softmax activation function, through which they were able to get a 98% accuracy. Hwang et al. proposed a DL-based Automated Detection Algorithm (DLAD) to categorize abnormal and normal radiograph images of thoracic disease (pneumonia, tuberculosis, active pulmonary, etc.) [26]. Gupta et al. proposed a deep network consisting of a dense block and 5 parallel classifiers for the identification of lung cancer through CT scan medical images and achieved an accuracy of 88.55% [27]. Fanelli et al. used public data from John Hopkins University to detect COVID-19 under different conditions [28].

Apostolopoulos et al. proposed VGG-19 for the detection of COVID-19, achieving an accuracy of 98.75% [29]. They collected datasets from Cohen's Github and pre-processed them by removing the redundancy of images. Butt et al. implemented ResNet-23 and ResNet-18 to detect chest infection using CT scan images and achieved an accuracy of 86.7% [30].

However, their approach cannot work in real-time systems due to their reduced time efficiency. Choi et al. proposed an approach based on logistic regression to detect COVID-19 on radiograph images [31]. The limitations of their approach include small data sizes.

Hameed et al. examined multi-system inflammatory syndrome in 35 children through chest radiographs and MRI images [32]. However, there are some limitations in the proposed system as it uses a lesser number of children in their experiment. Paul et al. applied a deep network on the COVID-19 chest radiograph dataset and achieved an accuracy of 89% [33]. However, there are some limitations as the availability of the COVID-19 radiograph is itself a barrier. Moreover, there is a lack of specificity in the model. This is because it is unable to differentiate COVID-positive CXR from the rest of the diseases, that is, alveolar pulmonary edema which causes air space opacities.

III. PROPOSED METHODOLOGY

The proposed approach used oGoogleNet which is our optimized version of oGoogleNet obtained by adding the convolution layer (7 7) and Max Pool Layer (3 3) along with the Stochastic Gradient Descent (SGD) optimizer and ReLU activation function. oGoogleNet is used for the identification of normal and abnormal chest radiographs. The oGoogleNet algorithm, introduced by Szegedy et al. [34], consists of 22 layers. The other most important characteristic is that it introduces the inception module.

The accuracy of a neural network can be increased by increasing the number of layers. In the proposed structure, one more convolution layer and another 3×3 max-pooling layer was added as shown in Figure

2. This exercise increased the feature extraction of data. In the methodology, oGoogleNet module worked as data was passed as input into six layers (four convolution layers (1 1), (3 3), (5 5), (7 7), and two max-pooling layers (3 3), (3 3). The results were then concatenated with the end layer of the inception module. The convolutional layers extract various spatial information from the input data. Whereas, the other two max-

pooling layers extract feature parameters by revising the channel and size of the input data. The design of the inception module is based on a nested network structure which makes it different from the conventional network. By applying the ReLU function, which is a linear activation function, on the (1 1) convolution layer, the complexity in the calculation is reduced as shown in Figure 2.

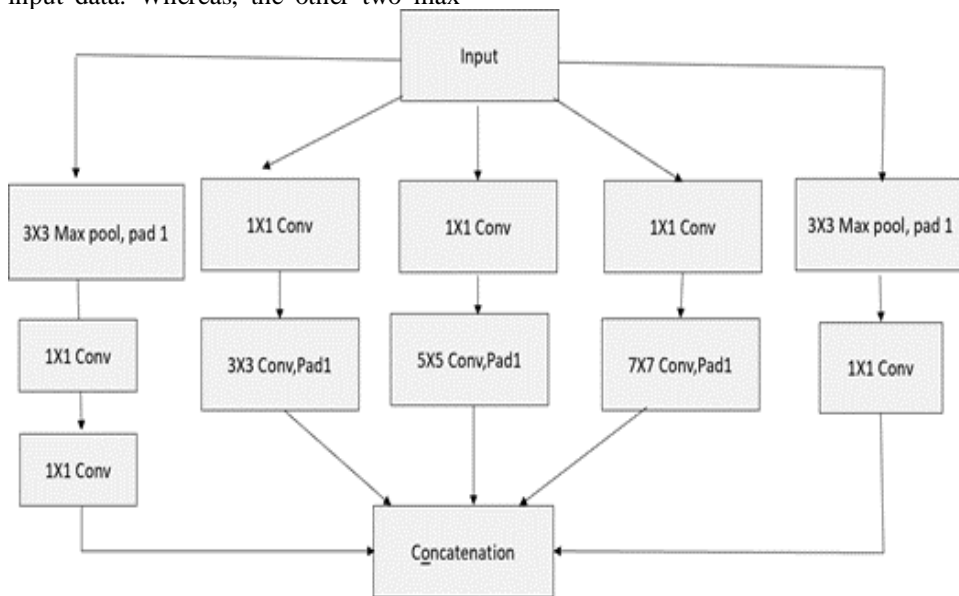


FIGURE 2. oGoogleNet model block

The applied parameters of oGoogleNet are given in Table II which consists of 30 layers and 10,479,110 parameters. oGoogleNet uses rectified linear unit (ReLU) activation function [35], which is fast in performance [36] and can easily be optimized due to its linear properties [36]. SGD optimizers simplify the learning rate as well as speed up convergence [37].

IV. DATASET

Eight different datasets were used. In these datasets, 5027 normal, 12071 pneumonia, and 777 COVID-19 images were found as shown in Table I. All the images were combined to create one data set containing a total of 12,389 chest radiographs with 7,825 abnormal (pneumonia, COVID-19) results and 4,564 chest radiographs with normal findings as shown in Figure 3.

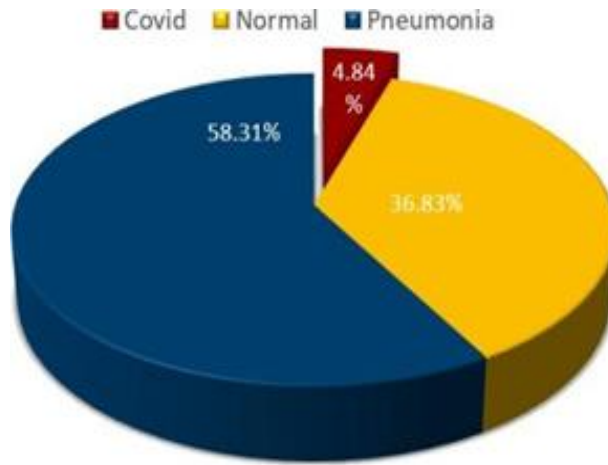


FIGURE 3. Statistical breakdown of chest radiographs

Since all datasets were taken from different sources, so the collected data was not uniform and the radiographs were not in the same format. Thus, all images were

converted into a similar size of 224*224. Data augmentation with rotation range 10 was also performed to increase the diversity of images.

TABLE I
STATISTICAL DESCRIPTION OF DATASETS WITH SOURCE

	COVID-19	Normal	Pneumonia
OCT CHXRAY [38]	-	1575	4266
COVID CHXRAY [39]	296	~	77
COVID RADIO DB [40]	219	1341	1345
COVID CHXRAY [40]	262	1583	4273
MNTG COUNTY [41]	-	58	80
SHENZHEN HOSPITAL [41]	~	326	336
CHESTXRAY [42]	~	144	144
NIH CHXRAY [43]	~	~	1500
Total	777	5027	12021

V.EXPERIMENTS AND DISCUSSION

oGoogleNet is compared with state-of-the-art existing deep networks including Alex-Net, Inception-V3, VGG-16, and ResNet-152 in terms of percentage accuracy and time efficiency on 12,389 chest

radiographs with a split ratio of 80 and

20. The accuracy and loss rate of oGoogleNet is shown in Figure 4. It can be inferred that the accuracy increases with the increase in the number of epochs and vice versa.

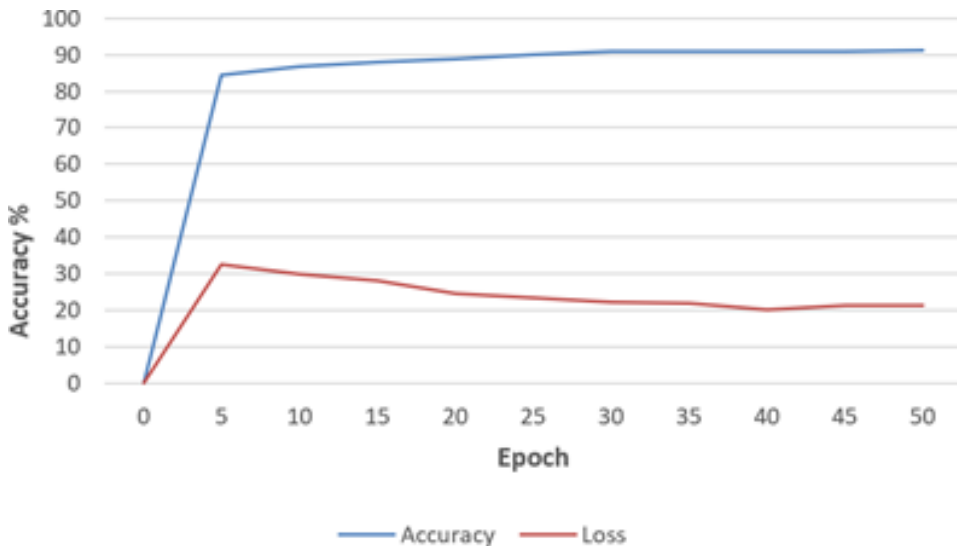
**FIGURE 4.** oGoogleNet accuracy and loss parameters

TABLE II

PARAMETRIC RESULTS OF VARIANTS OF THE PROPOSED AP PROACH

Optimizer	oGoogleNet-Adam	oGoogleNet-RMSProp	oGoogleNet-Adam	oGoogleNet-SGD	oGoogleNet-RMSProp	oGoogleNet
Accuracy	89.68	87.90	88.88	90.88	87.1	91.25
Time (sec)	1389	1357	1165	10020	1300	10080
Batch-Size	16	16	32	32	32	16

A. EXPERIMENT 1: COMPARISON IN TERMS OF ACCURACY

oGoogleNet outperforms the Alex-Net, Inception-V3, VGG-16, and ResNet-152 in terms of percentage accuracy as can be seen in Figure 5. The reason includes the addition of convolutional and pool layers in oGoogleNet architecture. The dataset of

radiographs has high intra-class variations due to the presence of various chest diseases including pneumonia, tuberculosis, COVID-19, and active pulmonary. The SGD, an important optimization module of oGoogleNet, speeds up the convergence method on this dataset.

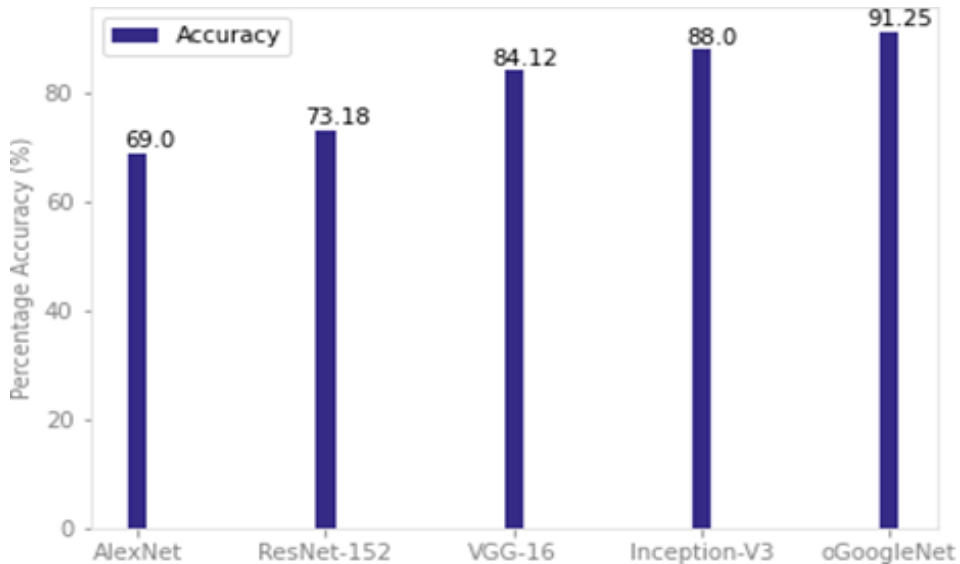


FIGURE 5. Comparison of oGoogleNet with existing state-of-the-art deep networks in terms of percentage accuracy with a split ratio of 80:20

B. EXPERIMENT 2: COMPARISON IN TERMS OF EXECUTION TIME

It can be observed in Figure 6 that oGoogleNet is 1.71, 1.75, 1.0 times faster

than VGG-16, ResNet-152, and AlexNet, respectively. oGoogleNet uses an SGD optimizer that increases the convergence of deep network on this dataset and hence, improves its time efficiency.

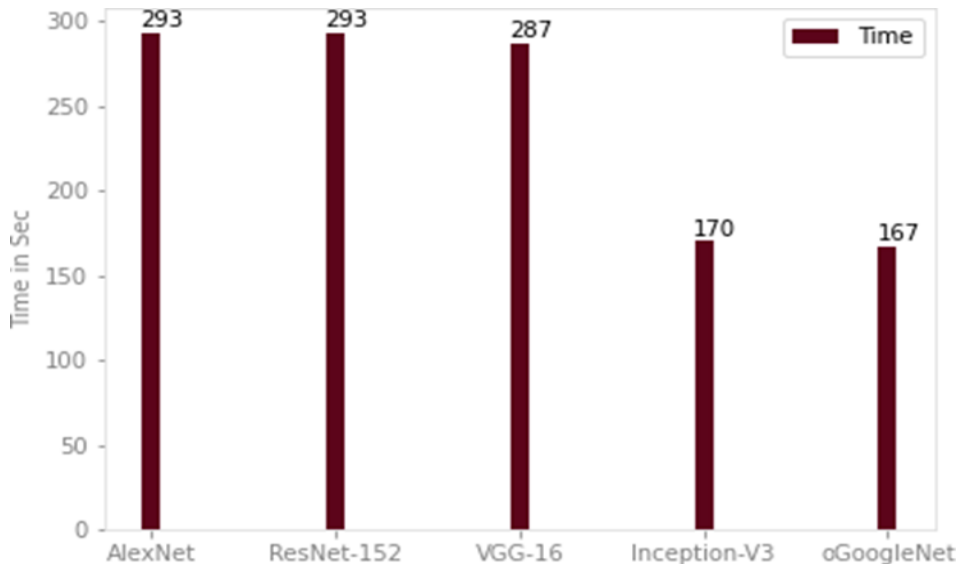


FIGURE 6. Comparison of oGoogleNet with existing state-of-the-art deep net-works in terms of time efficiency with a split ratio of 80:20

C. EXPERIMENT 3: VARIANTS OF PROPOSED APPROACH

Table II shows the comparison of oGoogleNet with its variants. These variants are obtained by changing the optimizers and batch size of oGoogleNet to see their effect in percentage accuracy and time efficiency. It can be observed that oGoogleNet outperforms its variants in terms of percentage accuracy. It exhibits comparable time efficiency as compared to oGoogleNet-SGD. Its other variants exhibit better time efficiency at the cost of percentage accuracy.

VI. CONCLUSION AND FUTURE WORK

The current study proposed a novel framework for the classification of pneumonia and COVID-19 chest radiographs using the optimized GoogleNet (oGoogleNet) model of DL. In this architecture, by adding one convolutional layer (7x7) and one MaxPool layer, feature extraction parameters were enhanced. The proposed architecture achieved 91.25% accuracy and outperformed other state-of-the-art architectures including AlexNet, VGG-16, Inception-V3, and ResNet-152. In future, the proposed model can be made more efficient both in terms of percentage accuracy and time efficiency. The addition of large data repositories would definitely help to improve the model.

CONFLICT OF INTEREST

The author of the manuscript has no financial or non-financial conflict of interest in the subject matter or materials discussed in this manuscript.

DATA AVAILABILITY STATEMENT

The data associated with this study will be provided by the corresponding author upon request.

FUNDING DETAILS

No funding has been received for this article.

REFERENCES

- [1] W. Kawohl and C. Nordt, "Covid-19, unemployment, and suicide." *Lancet Psych.*, vol. 7, no. 5, pp. 389–390, May 2020.
- [2] D. Altig *et al.*, "Economic uncertainty before and during the covid-19 pandemic," *Nation. Bureau Econ. Res.*, vol. 24, no. 2, pp. 27–38, Nov. 2020, doi: <https://doi.org/10.1016/j.jpubeco.2020.104274>.
- [3] C. Nordt, I. Warnke, E. Seifritz, and W. Kawohl, "Modelling suicide and unemployment: a longitudinal analysis covering 63 countries, 2000–11," *Lancet Psych.*, vol. 1, no. 3, pp. 239–245, Mar. 2015, doi: [https://doi.org/10.1016/S2215-0366\(14\)00118-7](https://doi.org/10.1016/S2215-0366(14)00118-7).
- [4] O. Coibion, Y. Gorodnichenko, and M. Weber, "Labor markets during the covid-19 crisis: A preliminary view (no. w27017)," working paper, Nat. Bureau Econ. Res., Massachusetts Avenue, USA. Available: <https://doi.org/10.3386/w27017>
- [5] J. Otte, J. Hinrichs, J. Rushton, D. Roland-Holst, and D. Zilberman, "Impacts of avian influenza virus on animal production in developing countries. *CABI Rev.*, vol. 80, no. 5, pp. 27–48, 2008.
- [6] R. F. Ceylan, B. Ozkan, and E. Mulazimogullari, "Historical evidence for economic effects of covid-19," *Eur. J. Health Econ.*, vol. 21, pp. 817–823, June 2020, doi: <https://doi.org/10.1007/s10198-020-01206-8>

- [7] G. Forchini *et al.*, “Report 28: Excess non-covid-19 deaths in England and Wales between 29th february and 5th june 2020,” *Lancet Psych.*, 2020, doi: <https://doi.org/10.25561/79984>.
- [8] H. Panwar, P. K. Gupta, M. K. Siddiqui, R. Morales-Menendez, and V. Singh, “Application of deep learning for fast detection of covid-19 in x-rays using nCOVnet,” *Chaos Solit. Fract.*, vol. 138, Sep. 2020, Art. no. 199044, doi: <https://doi.org/10.1016/j.chaos.2020.109944>.
- [9] T. Ai and Z. Yang, “Correlation of chest CT and RT-PCR testing in coronavirus disease 2019 (COVID-19) in China: A report of 1014 cases,” *Radiology*, vol. 296, no. 2, pp. E32–E40, Feb. 2020, doi: <https://doi.org/10.1148/radiol.2020200642>.
- [10] Y. Fang, H. Zhang, J. Xie, M. Lin, L. Ying, and P. Pang, “Sensitivity of chest CT for COVID-19,” *Compar. RT-PCR. Radiol.*, vol. 296, no. 2, pp. E115–E117, Feb. 2020, doi: <https://doi.org/10.1148/radiol.2020200432>.
- [11] J. P. Kanne, B. P. Little, J. H. Chung, B. M. Elicker, and L. H. Ketai, “Essentials for radiologists on covid-19: An update—radiology scientific expert panel,” *Radiology*, vol. 296, no. 2, pp. E113–E114, Feb. 2020, doi: <https://doi.org/10.1148/radiol.2020200527>.
- [12] S. S. Han *et al.*, “Deep neural networks show an equivalent and often superior performance to dermatologists in onychomycosis diagnosis: Automatic construction of onychomycosis datasets by region-based convolutional deep neural network,” *PloS One*, vol. 13, no. 11, Article ee0191493, Jan. 2018, doi: <https://doi.org/10.1371/journal.pone.0191493>.
- [13] M. M. Najafabadi, F. Villanustre, T. M. Khoshgoftaar, N. Seliya, R. Wald, and E. Muharemagic, “Deep learning applications and challenges in big data analytics,” *J. Big Data*, vol. 2, no. 16, pp. 1–21, Feb. 2015, doi: <https://doi.org/10.1186/s40537-014-0007-7>.
- [14] S. H. Yoo *et al.*, “Deep learning-based decision-tree classifier for covid-19 diagnosis from chest x-ray imaging,” *Front. Med.*, vol. 7, no. 13, pp. 427–427, July 2020, doi: <https://doi.org/10.3389/fmed.2020.00427>.
- [15] M. I. Razzak, S. Naz, and A. Zaib, “Deep learning for medical image processing: Overview, challenges and the future,” in *Classification in BioApps Automation of Decision Making*, N. Dey, A. Ashour, and S. Borra, Eds. Springer Nature, 2018, pp. 323–350.
- [16] V. Gulshan *et al.*, “Development and validation of a deep learning algorithm for detection of diabetic retinopathy in retinal fundus photographs,” *JAMA*, vol. 316, no. 22, pp. 2402–2410, 2016, doi: <https://doi.org/10.1001/jama.2016.17216>.
- [17] N. Bayramoglu and J. Heikkilä, “Transfer learning for cell nuclei classification in histopathology images,” presented at the Computer Vision – ECCV 2016 Workshops, Amsterdam, The Netherlands, October 8–10 and 15–16, 2016.
- [18] Y. Yuan and M. Q.-H. Meng, “Deep learning for polyp recognition in wireless capsule endoscopy images,” *Med. Phy.*, vol. 44, no. 4, pp. 1379–

- 1389, Feb. 2017, doi: <https://doi.org/10.1002/mp.12147>
- [19] Y. Peng and M. H. Nagata, "An empirical overview of nonlinearity and overfitting in machine learning using covid-19 data," *Chaos Solit. Fract.*, vol. 139, no. 22, Oct. 2020, Art. no. 110055, doi: <https://doi.org/10.1016/j.chaos.2020.110055>.
- [20] C Liu *et al.*, "Detecting tuberculosis in chest x- ray images using convolutional neural network," presented at 2017 IEEE International Conference on Image Processing (ICIP), Beijing, China, Sep. 17–20, 2017.
- [21] A. Esteva *et al.*, "Dermatologist-level classification of skin cancer with deep neural networks," *Nature*, vol. 542, pp. 115–18, Jan. 2017, doi: <https://doi.org/10.1038/nature21056>.
- [22] P. Rajpurkar *et al.*, "Chexnet: radiologist-level pneumonia detection on chest x-rays with deep learning," *arXiv Preprint*, 2017, doi: <https://doi.org/10.48550/arXiv.1711.05225>.
- [23] K. Murphy *et al.*, "Covid-19 on chest radiographs: A multireader evaluation of an artificial intelligence system," *Radiology*, vol. 296, no. 3, pp. E166–E172, May 2020, doi: <https://doi.org/10.1148/radiol.2020201874>.
- [24] N. Y. Ng *et al.*, "Imaging profile of the covid-19 infection: radiologic findings and literature review," *Radiol. Cardioth. Imag.*, 2, vol. 1, Feb. 2020, Art. no. e200034, doi: <https://doi.org/10.1148/ryct.2020200034>.
- [25] A. M. Alqudah, S. Qazan, and A. Alqudah, "Automated systems for detection of covid-19 using chest X-ray images and lightweight convolutional neural networks," *Res. Seq.*, 2020, doi: <https://doi.org/10.21203/rs.3.rs-24305/v1>.
- [26] E. J. Hwang *et al.*, "Development and validation of a deep learning-based automated detection algorithm for major thoracic diseases on chest radiographs," *JAMA Netw. Open*, vol. 2, no. 3, 2019, Art. no. e191095, doi: <https://doi.org/10.1001/jamanetworkopen.2019.1095>.
- [27] G. A. P. Singh and P. K. Gupta, "Performance analysis of various machine learning-based approaches for detection and classification of lung cancer in humans," *Neural Comput. Appl.*, vol. 31, pp. 6863–77, May 2018, doi: <https://doi.org/10.1007/s00521-018-3518-x>.
- [28] D. Fanelli and F. Piazza, "Analysis and forecast of covid-19 spreading in China, Italy and France," *Chaos Solit. Fract.*, vol. 134, May 2020, Art. no. 109761, doi: <https://doi.org/10.1016/j.chaos.2020.109761>.
- [29] I. D. Apostolopoulos and T. A. Mpesiana, "Covid-19: Automatic detection from X-ray images utilizing transfer learning with convolutional neural networks," *Phys. Eng. Sci. Med.*, vol. 43, pp. 635–640, Apr. 2020, doi: <https://doi.org/10.1007/s13246-020-00865-4>.
- [30] C. Butt, Gill, D. Chun, and B. Babu, "Deep learning system to screen coronavirus disease 2019 pneumonia," *Appl. Intell.*, vol. 53, p. 6863–6877, Apr. 2020, doi: <https://doi.org/10.1007/s10489-020-01714-3>.
- [31] H. Choi *et al.*, "Extension of coronavirus disease 2019 (COVID-19)

- on chest CT and implications for chest radiograph interpretation.” *Radiol. Cardioth. Imag.*, vol. 2, no. 2, Mar. 2020, Art. no. e200107, doi: <https://doi.org/10.1148/ryct.2020200107>.
- [32] S. Hameed *et al.*, “Spectrum of imaging findings on chest radiographs, US, CT, and MRI images in multisystem inflammatory syndrome in children associated with covid-19,” *Radiology*, vol. 298, pp. E1–E10, 2020, doi: <https://doi.org/10.1148/radiol.2020202543>.
- [33] H. Y. Paul, T. K. Kim, and C. T. Lin, “Generalizability of deep learning tuberculosis classifier to COVID-19 chest radiographs: New tricks for an old algorithm?” *J. Thor. Imag.*, vol. 35, no. 4, pp. W102–W104, July 2020, doi: <https://doi.org/10.1097/RTI.00000000000000532>.
- [34] C. Szegedy *et al.*, “Going deeper with convolutions,” in *Proc. IEEE Conf. Comput. Vision Patter Recog.*, Boston, MA, 2015, pp. 1–9.
- [35] V. Nair and G. E. Hinton, “Rectified linear units improve restricted Boltzmann machines,” in *Proc. 27th Int. Conf. Mach. Learn.*, Haifa, Israel, 2010, pp. 807–814.
- [36] Y. LeCun, Y. Bengio, and G. Hinton, “Deep learning,” *Nature*, vol. 521, pp. 436–444, May 2015, doi: <https://doi.org/10.1038/nature14539>.
- [37] Z. Zhang, “Improved Adam optimizer for deep neural networks,” presented at 2018 IEEE/ACM 26th International Symposium on Quality of Service (IWQoS), Banff, AB, Canada, June 4–6 2018, doi: <https://doi.org/10.1109/IWQoS.2018.8624183>.
- [38] D. Kermany, K. Zhang, and M. Goldbaum, “Labeled optical coherence tomography (OCT) and chest X-Ray images for classification,” *Mendeley Data*, vol. 2, no. 23, 2018, doi: <https://doi.org/10.17632/rscbjbr9sj.2>.
- [39] J. P. Cohen, P. Morrison, L. Dao, K. Roth, T. Q. Duong, and M. Ghassemi, “Covid-19 image data collection: Prospective predictions are the future,” *arXiv Preprints*, 2020, doi: <https://doi.org/10.48550/arXiv.2006.11988>.
- [40] K. Kerneler. “Starter: Chest X-ray images Pneumonia cfd22e54-7.” Kaggle.com. <https://www.kaggle.com/kerneler/starter-chest-xray-images-pneumonia-cfd22e54-7/data>.
- [41] S. Jaeger, S. Candemir, S. Antani, Y. X. J. Wang, P. X. Lu, and G. Thoma, “Two public chest X-ray datasets for computer-aided screening of pulmonary diseases,” *Quant. Imag. Med. Surg.*, vol. 4, no. 6, pp. 475–477, 2014, doi: <https://doi.org/10.3978/j.issn.2223-4292.2014.11.20>.
- [42] M. E. H. Chowdhury *et al.*, “Can AI help in screening viral and COVID-19 pneumonia?” *IEEE Access*, vol. 8, pp. 132665–132676, July 2020, doi: <https://doi.org/10.1109/ACCESS.2020.3010287>.
- [43] R. Summers, “NIH chest x-ray dataset of 14 common thorax disease categories.” NIH Clinical Center: Bethesda, MD, USA, 2019.